ELSEVIER

Applied Surface Science 116 (1997) 330–334

applied surface science

Electron–positron momentum density distribution in diamond

R.W.N. Nilen [a,*], S.H. Connell [a], W.G. Schmidt [b], D.T. Britton [c], W.S. Verwoerd [d], J.P.F. Sellschop [a], S. Shrivastava [e]

[a] *Schonland Research Centre for Nuclear Sciences, University of the Witwatersrand, PO Wits 2050, Johannesburg, South Africa*
[b] *Friedrich-Schiller-Universität Jena, Max-Wien-Platz 1, 07743 Jena, Germany*
[c] *Physics Department, University of Cape Town, Private Bag, Rondebosch 7700, South Africa*
[d] *Physics Department, University of South Africa, PO Box 392, Pretoria 0001, South Africa*
[e] *Physics Department, University of Transkei, Private Bag X1, Umtata, South Africa*

Received 2 June 1996; accepted 15 June 1996

Abstract

We have measured the momentum distribution of the electron–positron annihilating pair in diamond as a function of crystallographic orientation, using the Doppler broadening technique of positron annihilation spectroscopy. A 1% variation in the longitudinal projection of the momentum distribution was observed as the sample was rotated about the ⟨110⟩ axis. This anisotropic distribution shows an excellent agreement with a theoretical calculation performed based on two component density functional theory in the local density approximation. The results suggest strongly that the bulk positron density, though delocalized and inhomogeneous, has sufficient amplitude at the intra-bond regions such that the annihilation characteristics are dominated by the bond electron density and momentum distribution.

PACS: 78.70.B; 71.60; 71.15.M

Keywords: Doppler broadening; Diamond; Ab initio pseudopotential; Calculation

1. Introduction

Two configurations for the positron have been identified in diamond [1]. The first has an extremely short lifetime ($\tau \sim 115$ ps), a very large momentum spread (~ 3.5 keV) and accounts for as much as 80–95% of positrons implanted into the lattice. This state is commonly attributed to positron annihilation in bulk diamond. The second has a longer lifetime, a smaller momentum spread and accounts for the remaining implanted positrons. This state is linked to positron trapping and annihilation at lattice defects. The lifetime of this state is sample dependent, as is the lifetime of the bulk state to a much smaller degree. The transition from the first to the second state occurs at a rate of ~ 1 GHz and is well described by the two-state trapping model [2]. The models for the first configuration are still the subject of much debate. The difficulty has been to explain simultaneously the high initial population, extremely short lifetime and large momentum distribution of the state.

* Corresponding author. Tel.: +27-11-7163166; fax: +27-11-3392144; e-mail: connell@schonlan.src.wits.ac.za.

PII S0169-4332(96)01078-1

Positronium formation is not observed in the diamond lattice and this is well confirmed in age-momentum correlation (AMOC) experiments [3]. Indeed, AMOC measurements in diamond highlight the anomalous behavior of the positron in the diamond lattice when compared to other molecular insulators such as quartz and boron nitride, where positronium formation is known to occur [4]. Positronium formation cannot explain the high initial population of the first state or the fact that the short lifetime component is associated with an extremely large momentum distribution and vice versa. Recently, Fujii et al. [5] claim to have observed positronium formation in the grain boundaries between crystallites of natural diamond.

Puska et al. [6] calculated a lifetime of 114 ps for the positron in bulk diamond using their insulator model, which shows excellent agreement with many experimental values [3,7]. The calculation, based on the atomic polarizability of the host and the superposition of free-atom electron densities, highlighted the tendency of the positron to seek out into the interstitial regions of the perfect lattice (see [8] where the same is found for Si and GaAs). This suggested that the process responsible for the first configuration is annihilation in the interstitial regions of the lattice. However, the highly covalent nature of diamond leads to an extreme localization of the valence electron density in the intra-bond region, which is not well described by this calculation scheme [9]. To address this problem, an ab initio pseudopotential calculation was performed for delocalized positrons in diamond based on two component density functional theory and a local density approximation [10]. The results of the calculation indicate that the positron does indeed seek out into the interstitial regions but that the overlap of the electron–positron density peaks in the intra-bond region. The same was found for a molecular-orbital based calculation of the valence electron density distribution in the diamond lattice performed using the MOPAC code. These calculations suggest strongly that the bulk positron density, though delocalized and inhomogeneous, has sufficient amplitude at the intra-bond regions such that the annihilation characteristics are dominated by the bond electron density and momentum distribution.

It is therefore proposed that annihilation in the intra-bond region is the process dominantly responsible for the positron configuration in bulk diamond. Support for this conjecture is three-fold; the excellent agreement between the experimentally observed and theoretically calculated momentum distribution of the valence electrons in the carbon–carbon bond of various hydrocarbons [11], the theoretical simulation of the positron spectroscopic observables in diamond showing the pileup of the electron–positron overlap density at the intra-bond site [10], and the experiment reported in this paper. Intra-bond annihilation in semiconductors was first proposed by Dannefaer [12] where the valence electrons are treated as a free-electron gas.

The experiment reported in this paper was designed as a direct test of this intra-bond annihilation model. The very pronounced anisotropic spatial distribution of the valence electron density in diamond results in a highly anisotropic momentum distribution of the valence electron density. Assuming the positron to have fully thermalized prior to annihilation, a mapping of the momentum distribution of the electron–positron annihilating pair should reflect the bond symmetry of the lattice. The mapping was achieved by observing the variation in the Doppler broadening of the electron–positron annihilation radiation as the sample was rotated in the (110) plane. The (110) plane was chosen as it contains two $\langle 111 \rangle$ axes (the bonding direction) as well as the other major axes. The experimental results compare very well with the results of a two-component density functional theory calculation performed for delocalized positrons in diamond.

2. Experiment

The longitudinal momentum distribution of the electron–positron annihilating pair, P_L, results in a Doppler broadening of the annihilation gamma-rays (511 keV) given by

$$\Delta E = \tfrac{1}{2} c P_L \qquad (1)$$

where ΔE is the energy shift from 511 keV and c is the speed of light. Thus a measurement of this Doppler broadening as a function of the rotation of the sample provides a measure of the electron–positron momentum distribution.

The sample was formed with two rectangular diamonds cut from a single parent block along a (110) face. The dimensions of the diamonds ($4 \times 4 \times 3$ mm^3) ensured that all positrons annihilated in the diamond bulk. The diamond faces were polished to an optical quality finish with a diamond gritted disc to ensure a near perfect mating surface in the final stages of sample preparation. A 0.5 mm radius dimple was drilled into one of the diamonds with a YAG laser, into which 7 μCi of ^{22}Na was deposited. The water of crystallization was driven from this source deposit by baking the diamond at 300°C for 5 h. This method of sample preparation has proved successful in previous experiments [13], and reduces the fraction of positrons annihilating in the source. The two diamonds were then clamped together to form the diamond–source–diamond sandwich sample. The sample was held in a goniometer and aligned with the (110) plane of the diamond lattice normal to the detector face. A fine Laue orientation of the sample ensured that the sample-detector line was always coplanar with the (110) plane of the sample as it was rotated about its ⟨110⟩ axis. The detector, a Canberra HP(Ge) model 7229 (efficiency 36%), was placed 0.5 m from the sample to ensure an angular resolution of $\pm 3°$. The energy resolution of the spectrometer (Fig. 1) was approximately 1.2 keV at 511 keV.

The experiment took the form of standard Doppler broadening measurements as the sample was rotated through 360° about the ⟨110⟩ axis in 8° steps. This plane of rotation was specifically chosen to allow the ⟨111⟩, ⟨110⟩ and ⟨100⟩ projections of the valence electron momentum distribution to be observed. Fig. 2 is a view of the (110) plane of the diamond lattice. The black circles represent carbon atoms.

The Doppler broadening is measured by defining the S-parameter as the ratio of the area of the central interval of the 511 keV peak to the total peak area.

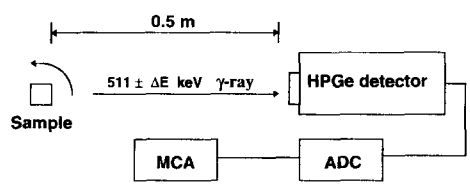

Fig. 1. The single detector Doppler broadening spectrometer with diamond sample rotation in the (110) plane.

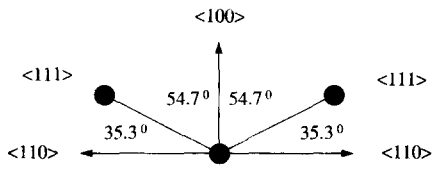

Fig. 2. The (110) plane in diamond.

The width of the central interval is chosen such that $S \sim 0.5$ and then fixed throughout the analysis. It is thus the variation in the S-parameter that is of interest. Approximately 2×10^6 counts in the 511 keV peak were taken in each measurement to ensure a relative error in the S-parameter of less than 0.5%. Each data point took about 10 h to collect, with the spectra being saved every hour to allow any drift to be removed with software during data analysis. The 661.7 keV line of a ^{137}Cs source was simultaneously measured to monitor the stability of the spectrometer. The background was modeled with an error function centered about 511 keV and subtracted before the analysis.

3. Theory

The electron–positron momentum density of delocalized positrons in bulk diamond was calculated using an ab initio pseudopotential approach. The calculation was based on two-component density-functional theory (DFT), a generalization of the one-component DFT that represents each species of particle by a distinct density (see e.g., Ref. [14] for a recent review). Assuming a plane wave, low momentum positron wave function, the positron density is negligible at every point of the infinite lattice and the electronic structure of the host remains unaltered. Therefore in this calculation, self-consistency was constrained to the calculation of the electronic ground state in the absence of positrons. The electronic ground state calculation rests on the local-density approximation (LDA) for the description of the many-body electron–electron interaction. The electron–ion interaction is accounted for by using fully separable, norm-conserving pseudopotentials [15] and is limited to a consideration of the valence electron density. The electron–positron interaction is

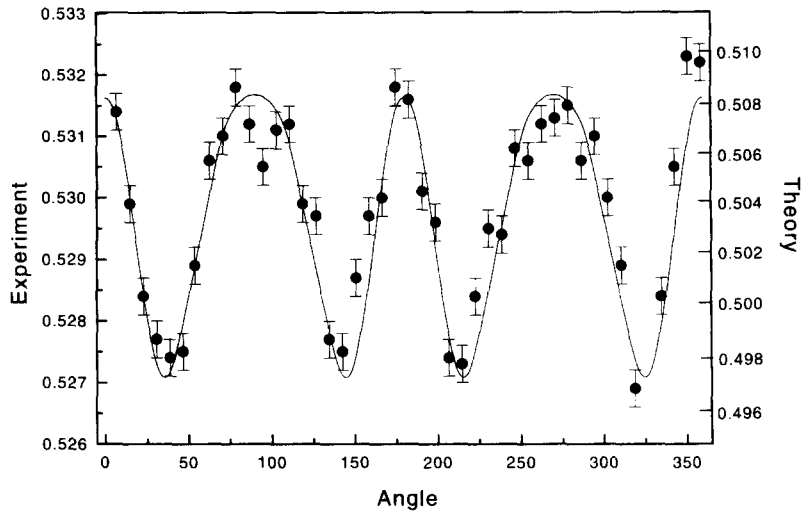

Fig. 3. S-parameter as a function of angle for both experiment and theory.

accounted for by using the Boronski–Niemenin parameterization of the electron–positron correlation potential [16], scaled to take into account the reduced screening due to the presence of the band gap in diamond. Taking the periodicity of the perfect crystal lattice into account, the momentum distribution can be written as [14]

$$\rho(P) = 2\sum_{n,k} f(n,k) \times \left| \int_{\Omega} \mathrm{d}r\, \mathrm{e}^{-iP\cdot r} \Psi_0^+(r)\Psi_{n,k}^-(r) \right|^2 \delta_{P,k+G} \quad (2)$$

where $f(n, k)$ is the Fermi function, $\Psi_0^+(r)$ is the ground state positron wave function, $\Psi_{n,k}^-(r)$ is the electron Bloch state with band index n and wave vector k, Ω is the volume of the primitive cell and G denotes a reciprocal lattice vector. Taking advantage of the plane wave representation of the single particle orbitals in our calculation, the above formula for the momentum distribution can be readily evaluated. To allow direct comparison with the experiment, a simulation of the angular dependence of the S-parameter was extracted from the momentum distribution. Details of the theoretical calculation are reported in [10].

4. Results

A 1% variation in the S-parameter was observed as the diamond was rotated about the ⟨110⟩ axis. The minima in the S-parameter at the ⟨111⟩ axes correspond to maxima in the Doppler broadening along these axes where the FWHM of the 511 keV peak was approximately 3.7 keV. The calculation predicted a 2.5% variation in the S-parameter and the FWHM of the 511 keV peak along the ⟨111⟩ axis to be approximately 3.8 keV, showing excellent agreement with experiment. The results of both the theoretical calculation and the experiment are plotted in Fig. 3.

The ⟨111⟩ axes lie at 35.3°, 144.7°, 215.3° and 324.7°; the ⟨110⟩axes lie at 0°, 180° and 360°; the ⟨100⟩ axes lie at 90° and 270°.

5. Discussion

A highly pronounced anisotropy in the valence electron momentum density distribution of diamond was clearly observed using the Doppler broadening technique of positron annihilation spectroscopy. The variation in the S-parameter reflects the anisotropic

momentum distribution of the valence electron density. This in turn reflects the anisotropic spatial distribution of the valence electron density, clearly illustrating the high degree of electronic localization in the bond region. The excellent agreement between theory and experiment suggests strongly that the bulk positron density, though delocalized and inhomogeneous, has sufficient amplitude at the intra-bond regions such that the annihilation characteristics are dominated by the bond electron density and momentum distribution. This intra-bond annihilation model explains simultaneously the extremely short lifetime, giant Doppler broadening and high intensity of the bulk positron configuration in diamond.

As the electron momentum distribution of many of the dominant defect types found in diamond, such as the monovacancy and nitrogen related centers, are expected to display the same symmetry as the diamond lattice, trapping at these defects cannot be neglected in this measurement. The quantitative difference between the theoretically predicted and experimentally observed variation in the S-parameter may be related to trapping at such defects, but is more likely the result of several experimental and theoretical factors. Experimentally, the energy resolution and angular resolution of the spectrometer are the main factors that contribute to the difference. Theoretically, the neglect of core-electron annihilation and the extension of LDA (including the reduced screening factor) to a large band gap material such as diamond are important considerations. The use of pseudopotentials induces an uncertainty in the high momentum components which may also lead to some degree of disagreement. More interestingly, the quantitative difference may indicate incomplete thermalization of the positron in the diamond lattice, as a randomly oriented positron momentum vector would have the net effect of washing out the observed anisotropy.

Acknowledgements

The authors would like to thank Messrs. de Beers Industrial Diamond Division (Pty) Ltd. for support, in particular in the provision of materials.

References

[1] M. Koch, K. Maier, J. Major, A. Seeger, J. Sellschop, E. Sideras-Haddad, H. Stoll and S. Connell, Mater. Sci. Forum 105–110 (1992) 671.
[2] A. Seeger, J. Phys. F (Met. Phys.) 3 (1973) 248.
[3] H. Stoll, M. Koch, U. Lauff, K. Maier, J. Major, A. Seeger, P. Wesolowski, I. Billard, J.Ch. Abbe, G. Duplatre, S. Connell, J. Sellschop, E. Sideras-Haddad, K. Bharuth-Ram and H. Harichuran, in: Proc. 5th Int. Workshop on Slow-Positron Beam Techniques for Solids and Surfaces, Eds. E. Ottewitte and A. Weiss, Vol. 303 (Am. Inst. Phys. Conf. Proc., New York, 1994) p. 179.
[4] H. Stoll, M. Koch, U. Lauff, K. Maier, J. Major, H. Schneider, A. Seeger and A. Siegle, Appl. Surf. Sci. 85 (1995) 17.
[5] S. Fujii, Y. Nishibayashi, S. Shikata, A. Uedono and S. Tanigawa, J. Appl. Phys. 78(3) (1995) 1510.
[6] M. Puska, S. Makinen, M. Manninen and R. Nieminen, Phys. Rev. B 39 (1989) 7666.
[7] S. Dannefaer, P. Mascher and D. Kerr, Diamond Rel. Mater. 1 (1992) 407.
[8] M. Saito, A. Oshiyama and S. Tanigawa, Phys. Rev. B 44 (1991) 10601.
[9] M. Puska, O. Jepsen, O. Gunnarsson and R. Nieminen, Phys. Rev. B 34 (1986) 2695.
[10] W. Schmidt and W. Verwoerd, Phys. Lett. A., to be published.
[11] S. Chuang, W. Holt and B. Hogg, Can. J. Phys. 46 (1968) 2309.
[12] S. Dannefaer, J. Phys. C (Solid State Phys.) 15 (1982) 599.
[13] H. Harichuran, MS Thesis, University of Durban Westville (1993).
[14] M. Puska and R. Nieminen, Rev. Mod. Phys. 66 (1994) 841.
[15] X. Gonze, R. Stumpf and M. Scheffer, Phys. Rev. B 44 (1991) 8503.
[16] E. Boronski and R.M. Nieminen, Phys. Rev. B 34 (1986) 3820.